Evidence for nanoscale phase separation of stressed–rigid glasses

2003 J. Phys.: Condens. Matter 15 S2397

(http://iopscience.iop.org/0953-8984/15/31/315)

INSTITUTE OF PHYSICS PUBLISHING JOURNAL OF PHYSICS: CONDENSED MATTER

J. Phys.: Condens. Matter **15** (2003) S2397–S2411 PII: S0953-8984(03)62843-2

Evidence for nanoscale phase separation of stressed–rigid glasses

S Mamedov, D G Georgiev, Tao Qu and P Boolchand

Department of Electrical, Computer Engineering and Computer Science, University of Cincinnati, Cincinnati, OH 452221-0030, USA

E-mail: pboolcha@ececs.uc.edu

Received 29 April 2003
Published 23 July 2003
Online at stacks.iop.org/JPhysCM/15/S2397

Abstract

Ternary $(Ge_2X_3)_x(As_2X_3)_{1-x}$ glasses with X = S or Se are of interest because they span a mean coordination number r in the $2.40 < r < 2.8$ range that is characteristic of *stressed–rigid* glasses. We have examined X = S glasses in Raman scattering and T-modulated differential scanning calorimetry measurements over the $0 < x < 1.0$ range. Glass transition temperatures, $T_g(x)$, increase monotonically in the $0 < x < 0.8$ range and decrease thereafter ($0.8 < x < 1$) to display a global maximum near $x = 0.8$. Raman scattering provides evidence of sharp modes of As_4S_4 and As_4S_3 monomers, with scattering strength of these modes showing a global maximum near $x = 0.3$ and 0.5 respectively. The results suggest that at low x ($0 < x < 1/2$), addition of Ge_2S_3 to the As_2S_3 base glass results in insertion of $Ge(S_{1/2})_4$ tetrahedra in the $As(S_{1/2})_3$-based backbone as compensating As-rich monomers segregate from the backbone to deliver the requisite S. At higher x ($0.4 < x < 0.8$), the Ge_2S_3 additive continues to enter the glass in a *majority* $(As_2S_3)(GeS_2)$ backbone and several minority nanophases including an ethane-like $Ge_2(S_{1/2})_6$ and a distorted rock-salt-like GeS. In the $0.8 < x < 1$ range, the nanophases grow qualitatively at the expense of the backbone as T_g values decrease and the end-member composition ($x = 1$) is realized. Heterogeneity of glasses near $x = 1/2$ or mean coordination, $r = 2.60$ derives intrinsically from the presence of several minority nanophases and a majority backbone showing that *stressed–rigid* networks usually phase separate on a nanoscale.

(Some figures in this article are in colour only in the electronic version)

1. Introduction

1.1. Floppy, intermediate and stressed–rigid phases in network glasses

The discovery of *thermally reversing windows* [1] in chalcogenide glasses represents a recent development in glass science. It has led to the recognition of *self-organization* in disordered networks [1–3] with consequences overflowing to oxide glasses [4], biological networks [5] and

electronic ones [6] including high-T superconductivity. In several binary and ternary systems, one has observed [7–14] glass transitions (T_g) to become almost completely *thermally reversing* in character over a range of chemical compositions. Specifically, the *non-reversing enthalpy* associated with T_g, accessed from temperature-modulated differential scanning calorimetry (MDSC), is found to nearly *vanish* for these compositions. Furthermore, these thermal measurements complemented by Raman scattering ones have revealed that *thermally reversing windows* usually open [7, 10, 14] between mechanically *floppy* and *stressed–rigid* phases of glasses. Glass compositions in these windows define *intermediate phases* [1–3] that are thought to represent *stress-free* (*self-organized*) phases of disordered networks. In select glass systems that possess onefold coordinated atoms (such as halogen atoms that produce dangling ends) the windows *collapse* to a solitary composition, and one observes [12, 13] a sharp *floppy* to *stressed rigid* transition near a mean coordination number, $r = 2.34$. The latter observations are in excellent agreement with the Phillips–Thorpe rigidity transition [15, 16] extended to networks including dangling ends [17, 18].

These new results on elastic phase transitions in network glasses have rekindled interest on a related issue, the microscopic origin of anomalies observed in glasses near a mean coordination $r = 2.60$. Several years ago, Keiji Tanaka [19] suggested that anomalies in physical properties (including T_g) of chalcogenide glasses near $r = 2.60$ may result from a *floppy* to *rigid* transition involving a change of network dimensionality.

In recent years, new ideas to understand the structural origin of T_g have emerged from stochastic agglomeration theory [20, 21]. In select cases the theory has predicted parameter-free compositional trends in T_g particularly in the stochastic regime of agglomeration. These predictions are in excellent accord with experimental results [9, 11, 12, 22, 23] and serve to demonstrate that T_g is an intimate reflection of network global connectivity. The global maximum in T_g in binary glasses near $r = 2.60$ could then result from an intrinsic nanoscale phase separation (NSPS) of *stressed rigid* networks. Glass compositions at $r < 2.60$ could be fully while those at $r > 2.60$ partially polymerized and separate into nanophases leading to anomalies in several physical properties. Such a physical picture appears appropriate to the case of binary Ge–Se and Ge–S glasses near the chemical threshold ($r = 2.67$) as was discussed recently [22–24] from thermal and spectroscopic measurements.

In the present work we have examined the case of ternary $(Ge_2X_3)_x(As_2X_3)_{1-x}$ glasses that have been the subject of several previous studies [25–27]. These glasses are of interest because, in principle, they span a mean coordination number range of $2.4 < r < 2.80$ that is characteristic of *stressed–rigid* networks. To estimate r, we take the coordination numbers of S, As and Ge to be two, three and four respectively. The paper is organized as follows. After presenting MDSC and Raman scattering results in section 2, we proceed to discuss the underlying molecular structures suggested by these results in section 3. The principal conclusions are summarized in section 4. The present results show that $(Ge_2S_3)_x(As_2S_3)_{1-x}$ glasses are partially polymerized, and consist of characteristic nanophases that contribute to heterogeneity of their molecular structures, particularly near $x = 1/2$ corresponding to $r = 2.60$. Nanoscale phase separation provides a better basis for understanding the network anomalies near $r = 2.60$ than a rigidity transition involving a change in network dimensionality [19].

2. Experimental details

2.1. Sample synthesis and experimental procedure

99.999% As_2S_3, Ge and S lumps from Cerac Inc. were used as starting materials. The materials were reacted in evacuated ($<5 \times 10^{-7}$ Torr) fused quartz ampoules of 5 mm id and 1 mm

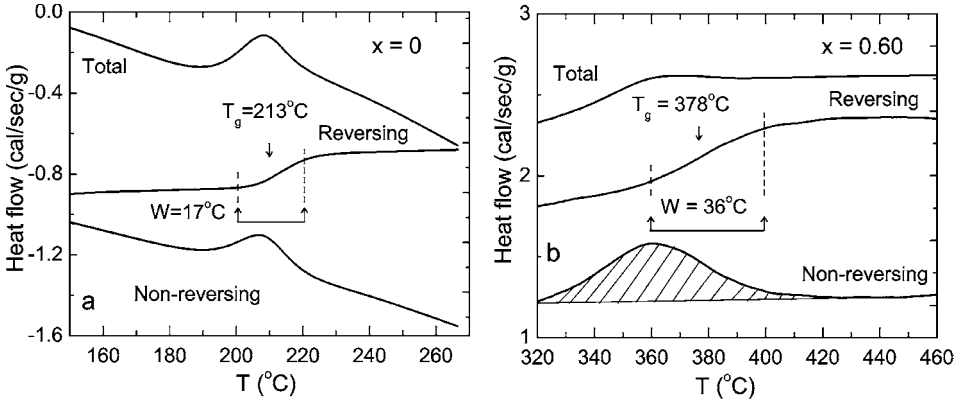

Figure 1. MDSC scans of $(As_2S_3)_{1-x}(Ge_2S_3)_x$ bulk glasses taken at a scan rate of 3 °C min^{-1} and a modulation rate 1/100 s for a sample at (a) $x = 0$ and (b) at $x = 0.60$. The three curves in each panel give the total, reversing and non-reversing heat flow recorded going up in temperature in a model 2920 unit from TA instruments. The width W of the glass transition accessed from the reversing heat flow is 17 °C for the $x = 0$ sample, and 36 °C for the $x = 0.60$ sample.

wall thickness. The starting materials were slowly taken up to 920 °C, and melts homogenized for an extended period (48 h) in a rocking furnace at that temperature. Melt temperatures were then lowered to 50 °C above the liquidus, and equilibrated for a few hours before a water quench. Samples possessed deep red colour.

Raman spectra of freshly quenched glasses were taken with a triple monochromator model T64000 unit from Jobin Yvon Inc., using 647 nm excitation in a backscattering configuration. Raman measurements of 3 week aged samples were taken with a LabRam system from Jobin Yvon Inc. using 633 nm excitation from a He–Ne laser. Spectra were acquired at 1 cm^{-1} resolution. The latter results yielded significantly higher signal/noise ratios and are presented here. Samples were aged for 1 week at room temperature prior to examination in T-modulated DSC (MDSC) measurements using a model 2920 unit from TA Instruments Inc. MDSC offers the advantage to decompose the total endothermic heat flow at T_g (measured in DSC) into a non-reversing (kinetic) and a reversing (thermodynamic) component by programming a sinusoidal T-variation over a linear T-ramp [9, 22, 23].

2.2. Temperature-modulated differential scanning calorimetry (MDSC)

Figure 1(a) displays the total, non-reversing and reversing heat flows for a glass sample at $x = 0$. Noteworthy in these scans is the fact that the equipment baseline is sloping down at higher temperatures as reflected in the total and non-reversing heat flow signals. The reversing heat-flow signal, on the other hand, always sits on a *flat* baseline in this method. The step size in the reversing heat flow permits fixing ΔC_p, while the inflexion point serves to define T_g of 220 °C. The onset and end of the glass transition as determined by a change in slope fixes the width of the transition, W, at 17 °C. Figure 1(b) shows scans observed for a glass sample at $x = 0.60$. In relation to the sample at $x = 0$, we find T_g to increase to 378 °C, and W to nearly double (36 °C). The typical error bar on T_g is 2 °C and on W about 4 °C.

Figure 2 provides a summary of MDSC results. Figure 2(a) shows the observed $T_g(x)$ variation. T_g values are found to increase monotonically in the $0 < x < 0.8$ range, and to decrease thereafter ($0.8 < x < 1.0$) to show a global maximum of 446 °C near $x = 0.80$. The latter T_g is close to that of GeS_2 glass [18] of 508 °C. Widths of the glass transition, $W(x)$,

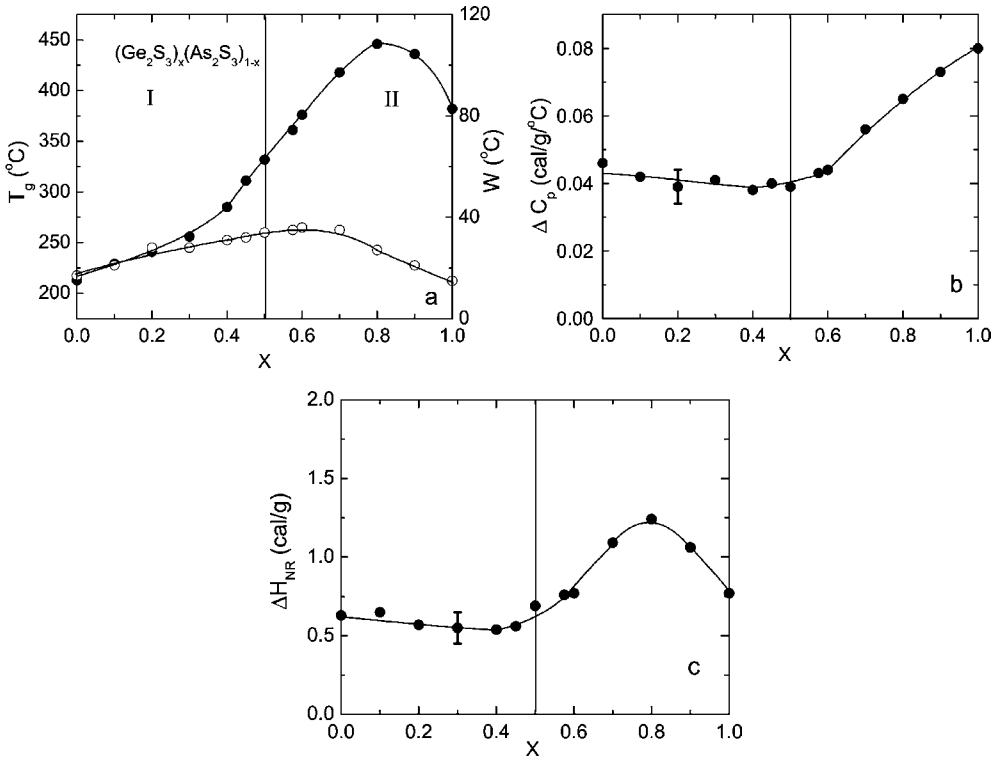

Figure 2. Summary of MDSC results on $(As_2S_3)_{1-x}(Ge_2S_3)_x$ bulk glasses showing compositional trends in (a) glass transition temperature, T_g (●), and width of T_g, W (○), (b) the specific heat jump from the reversing heat flow, ΔC_p, and (c) the shaded integrated area from the reversing heat flow signal, ΔH_{nr}.

also appear in figure 2(a) and show a global maximum near $x = 0.60$. For completeness, we include in figures 2(b) and (c) trends in $\Delta C_p(x)$ obtained from the reversing heat flow, and those in $\Delta H_{nr}(x)$ from the non-reversing heat flow, respectively. We find both $\Delta H_{nr}(x)$ and T_g to show a global maximum near $x = 0.8$. $\Delta C_p(x)$ inferred from the reversing heat flow, on the other hand, continues to increase monotonically with x. We shall discuss these results in section 3.

2.3. Raman scattering

Figure 3 provides an overview of the observed Raman lineshapes of samples taken 3 weeks after a water quench. Raman spectra of *fresh* samples were identical to these. The principal features of these results are as follows. In the low x range ($0 < x < 1/2$), the observed lineshapes reveal growth in scattering strength of eight low-frequency modes labelled ν_1–ν_8. These modes are more clearly displayed in figures 4(a) and (b), that show blow-ups of the two rectangular segments of figure 3. The narrow modes can be identified with intramolecular vibrations of As_4S_4 and As_4S_3 monomers (table 1). In this group of modes of particular interest are the ones ν_6 and ν_8 that have contributions exclusively from As_4S_4 and As_4S_3 monomers respectively. The observed lineshapes were fitted as a superposition of eight Gaussians keeping their widths, centroids and intensities as variables. Compositional trends in normalized scattering strengths, $I(x)$, reveal that concentrations of As_4S_4 monomers (mode ν_6) and of As_4S_3 monomers (mode ν_8) display maxima near $x = 0.3$ and 0.5 respectively (figure 4(c)). We also note that feature

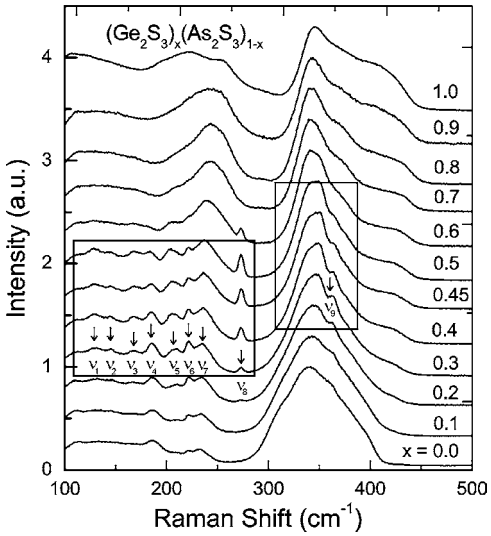

Figure 3. Raman lineshapes in $(As_2S_3)_{1-x}(Ge_2S_3)_x$ bulk glasses at indicated compositions showing growth of sharp modes due to As_4S_4 and As_4S_3 monomers near $x = 1/2$. A blow-up of the two rectangular panels highlights the sharp modes in figures 4(a) and (b) respectively.

Table 1. Raman frequencies observed in α- and β-As_4S_4, α-As_4S_3 and glassy As_2S_3.

α-, β-As_4S_4	As_4S_3 cryst.	As_2S_3 glass [19]
376	375	
370	370	373
355	354	352
344	340	334
	268—ν_8	
222—ν_6	217[a]	227
215/212		206
193	197	195
184	181	
173	175	
157		
144	142	

[a] The scattering strength of the 217 cm^{-1} mode is weak. The mode ν_6 can be regarded as a signature of As_4S_4 monomers.

$\nu_9 = 375$ cm^{-1} as a shoulder to the principal band centred near 340 cm^{-1} (figure 4(b)) also grows in scattering strength with x to show a global maximum near $x = 0.30$. This particular mode is ascribed to As_4S_4 monomers as discussed recently by Georgiev *et al* [28].

In the high x range ($1/2 < x < 1$), the observed lineshapes are altogether quite different. The narrow modes of the As-rich monomers steadily disappear as $x > 1/2$. Furthermore, near the composition $x = 0.7$, one observes a broad band centred near $\nu_7 = 250$ cm^{-1}, and modes near 344, 370 and 460 cm^{-1}. These vibrational modes are characteristic [23, 29] of a $Ge_{0.35}S_{0.65}$ glass, i.e. a slightly Ge-rich GeS_2 glass. The three modes at 344, 370 and 460 cm^{-1} are assigned [30, 31] to corner-sharing (CS), edge-sharing (ES) and high-frequency scissors (F_2) modes of $Ge(S_{1/2})_4$ tetrahedra. The 250 cm^{-1} mode represents [22, 30] a vibration of an ethane-like Ge_2S_6 nanophase that segregates from the GeS_2-like phase. The CS mode near

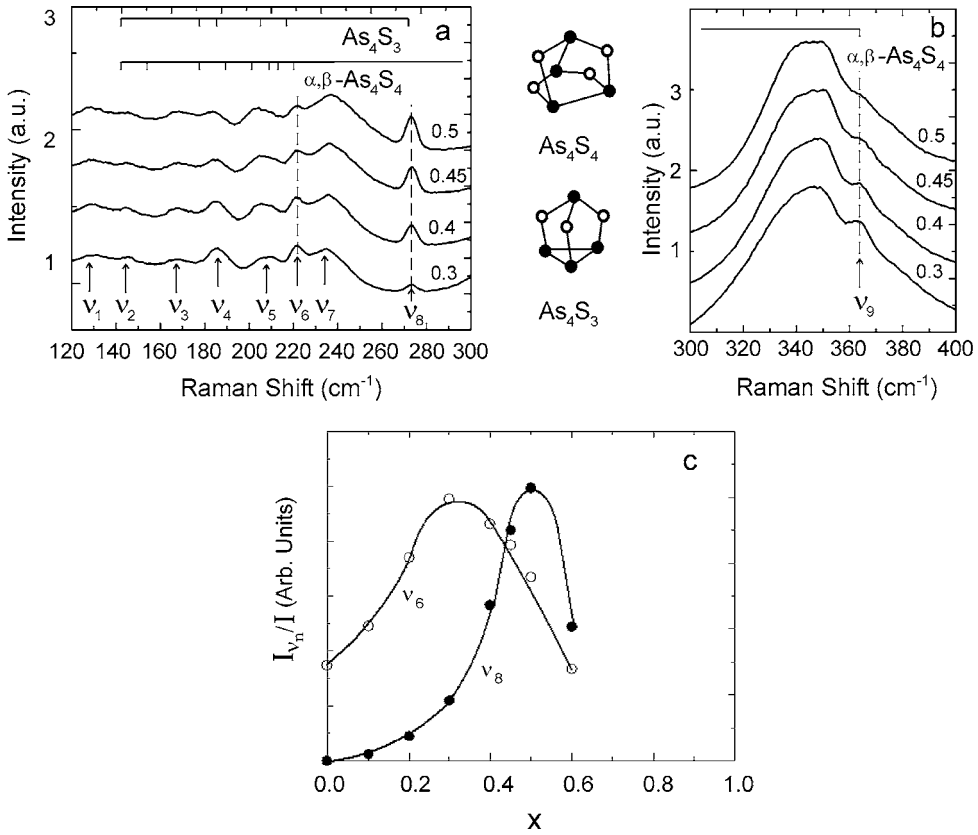

Figure 4. Panels (a) and (b) show the nine modes labelled $\nu_1 \cdots \nu_9$ which are traced to the presence of As_4S_4 monomers, As_4S_3 monomers and ethane-like (ν_7) units in the glasses. The expected mode frequencies for the monomers appear as a bar chart on top. The frequencies of the monomers were taken from [40] and [41]. (c) Compositional trends in scattering strength of ν_6 and ν_8 modes identified exclusively with As_4S_4 and As_4S_3 monomers respectively.

340 cm^{-1} in the ternary glass near $x = 0.5$ is rather broad in relation to that in GeS_2 glass, and most likely has overlapping contributions from modes of As pyramids and Ge tetrahedra.

Raman spectra of ternary glasses at higher x (>0.8) begin to acquire features that we associate with the end-member composition $x = 1$, i.e., Ge_2S_3 glass [29, 31]. These features include

(a) considerable reduction of Raman scattering as the optical gap of the glasses reduces, thereby resulting in significant loss of resonant enhancement,
(b) appearance of broad bands near 200 and 400 cm^{-1} and
(c) considerable reduction in scattering strength near 330 cm^{-1}.

These Raman lineshape features are related to the global maximum of T_g near $x = 0.8$. The underlying structural changes will be discussed in the next section.

3. Discussion

We begin our discussion of the results by first reviewing the glass forming tendency in binary As–S glasses, and then proceed to the present ternary.

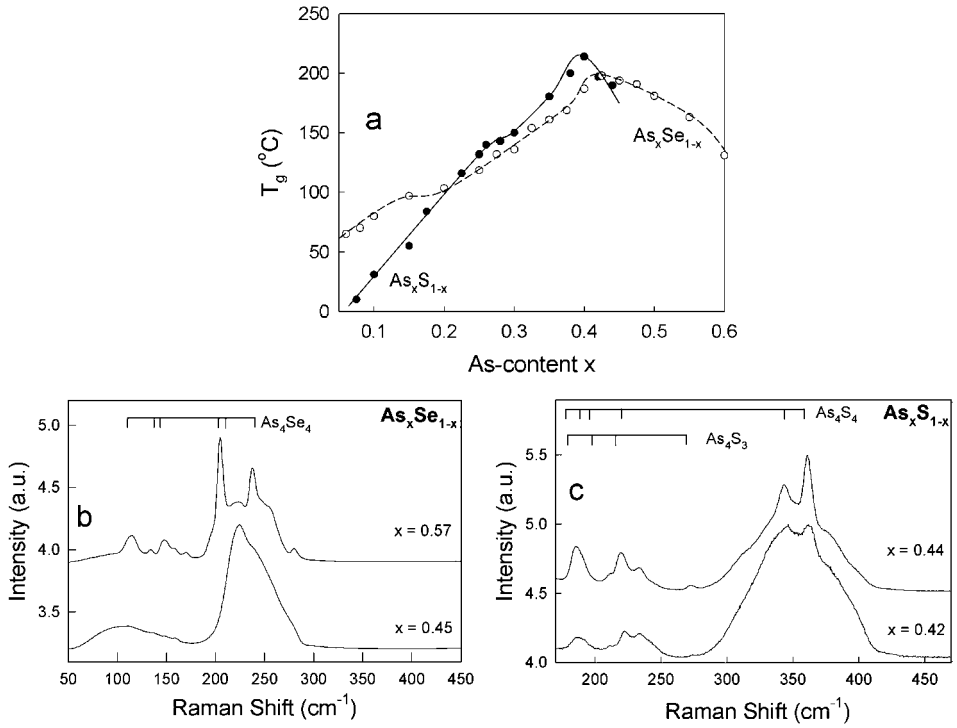

Figure 5. (a) Compositional trends in T_g for binary As_xS_{1-x} and As_xSe_{1-x} bulk glasses showing global maxima near the chemical threshold of $x = 2/5$. Note that selenide glasses can be made up to $x = 0.6$, but sulfide glasses only up to 0.45. Raman scattering in (b) As_xSe_{1-x} glasses at $x = 0.45$ and 0.57 and (c) As_xS_{1-x} glasses at $x = 0.42$ and 0.44.

3.1. Glass forming tendency and molecular structure of binary As–S glasses

Since the early work of Myers and Felty [32] and others [33, 34], it has been known that bulk glass formation in As_xSe_{1-x} extends over a wide range, $0 < x < 0.60$, but in corresponding sulfides, As_xS_{1-x}, it abruptly ceases once $x > 0.45$. Figure 5(a) reproduces compositional trends in glass transition temperatures $T_g(x)$ in both binary glasses. One observes a global maximum in $T_g(x)$ near the chemical threshold of $x = 2/5$. The molecular origin of the behaviour can be traced to cross linking of chalcogen-rich chains as As is alloyed, and to the formation of As_4Se_4 monomers in the former and As_4S_4 and As_4S_3 monomers in the latter once $x > 2/5$ [21, 28]. Formation of monomers leads to a progressive loss of the $As(X_{1/2})_3$ backbone that is reflected in a catastrophic loss of global connectivity. The rapid reduction of T_g and eventual loss of glass formation, once $x > 0.45$ in the sulfides, are directly related to a break-up of the network.

There is an important difference in the way monomers appear in binary As–Se glasses from those in As–S ones, however. In the As–Se binary, As–As bonds first emerge in polymeric units composed of ethylene-like $As_2(Se_{1/2})_4$ units, and then transform [35, 36] into As_4Se_4 monomers at higher $x > 0.50$. The view is corroborated from Raman spectra of these glasses (figures 5(b) and (c)) that reveal sharp bands once $x > 0.50$. On the other hand, in the As–S binary [28, 37] monomers grow even when x is near two-fifths. It appears that the polymeric form of an ethylene-like $As_2(S_{1/2})_4$ unit with the more ionic S is chemically *unstable*, and does not form. On chemical grounds, one expects the more electronegative sulfur to form

the monomers with S lone pair electrons dressing cluster surfaces. These differences of molecular structures between As–S and As–Se glasses have an important bearing on structure of corresponding ternary Ge–As–S and Ge–As–Se glasses as we shall see next.

3.2. Molecular structure of As-rich glasses: region I ($0 < x < 0.5$)

Trivalent As in a chalcogen-rich glass forms threefold coordinated pyramidal $As(S_{1/2})_3$ units corresponding to As_2S_3 stoichiometry. On the other hand, tetravalent Ge forms fourfold coordinated $Ge(S_{1/2})_4$ tetrahedra corresponding to GeS_2 stochiometry. Thus, when Ge_2S_3 is alloyed with As_2S_3 glass, there is *insufficient* amount of S per Ge atom to form $Ge(S_{1/2})_4$ tetrahedra. The electronegativity [38] difference between Ge (2.01) and S (2.56) exceeds that between As (2.18) and S (2.56). These charge transfer effects suggest that S will first select to covalently bond with Ge rather than As atoms to lower free energy of the alloyed network. Thus, addition of Ge_2S_3 to As_2S_3 base glass will lead Ge tetrahedra to be formed in the As-based backbone provided a compensating As-rich phase nucleates to deliver the requisite amount of S. In this context, it is useful to consider the following chemical reactions that will provide the basis to understand the molecular structure of the glasses. One of the possible As-rich phases to nucleate consists of As_4S_4 monomers,

$$2As_2S_3 = As_4S_4 + 2S \tag{1a}$$

$$2Ge_2S_3 + 2S = 4GeS_2 \tag{1b}$$

leading to the reaction

$$2Ge_2S_3 + 2As_2S_3 = As_4S_4 + 4GeS_2. \tag{1c}$$

Here reaction (1*a*) provides for some decomposition of the backbone to release S and the formation of As_4S_4 monomer, while reaction (1*b*) converts the Ge sesquisulfide to GeS_2 units with the released S.

A parallel set of reactions can be expected with formation of As_4S_3 monomers,

$$2As_2S_3 = As_4S_3 + 3S \tag{2a}$$

$$3Ge_2S_3 + 3S = 6GeS_2 \tag{2b}$$

leading to the following reaction:

$$3Ge_2S_3 + 2As_2S_3 = As_4S_3 + 6GeS_2. \tag{2c}$$

Reaction (2*b*) permits conversion of the Ge sequisulfide into the disulfide, and results in the additive being alloyed with the base glass by reaction (2*c*). These reaction equations also suggest that if either reaction (1*c*) or (2*c*) were to take place in these glasses one would expect the former to maximize near $x = 1/2$ and the latter near $x = 0.6$. This is almost the case in our experiments but not quite (figure 4(c)), a point we shall return to comment on later.

A perusal of the equilibrium phase diagram of the As–S binary unequivocally shows that the only known As-rich phases (containing As–As bonds) to exist are As_4S_4 and As_4S_3 monomers (figure 4(b)). Crystalline As_4S_4 exists as a molecular solid comprising the monomers in several polymorphic phases [39, 40]. As_4S_3 monomers [41] have P_4Se_3 counterparts and consist of a cage having a triangular base of As (or P) atoms and an apical As (or P) atom that are bridged by triads of sulfur as shown in figure 4(b) inset. Thus, the only known As-rich phases that can form in the present ternary glasses consist of As_4S_4 and As_4S_3 monomers. For these reasons, reactions (1*c*) and (2*c*) become central to understand the chemical alloying process in the present ternary glasses.

The Raman spectra (figure 4(a)) provide evidence for eight sharp modes (ν_n, $n = 1$–8) that constitute evidence in part for the As-rich molecular species formed in these glasses. Parallel

Raman results were reported by Arsova *et al* [26]. The sharpness of the modes suggests that these molecular species are decoupled from the backbone. Particularly noteworthy is the fact that the first unit to nucleate in the glasses is the As_4S_4 monomer already near $x = 0$ [28, 42], and its concentration maximizes near $x = 0.30$ (figure 4(c)). The As_4S_3 monomer apparently nucleates a little later near $x = 0.2$, and its concentration goes through a global maximum near $x = 0.5$ (figure 4(c)). The formation of these cages releases S and permits Ge_2S_3 additive to alloy with the $As(S_{1/2})_3$ backbone in the form of GeS_2 tetrahedra. A consequence of such alloying is that the global connectivity (as fourfold Ge replaces threefold As) of the backbone systematically increases. The latter is reflected in T_g values that increase from 210 °C at $x = 0$ to 446 °C at $x = 0.8$ (figure 2(a)). These results are in harmony with the structural interpretation of T_g as a measure [21] of the global connectivity of a glass network.

The physical picture of glass structure evolving in *region I* is that of a backbone consisting of GeS_2–As_2S_3 units, with concentrations of decoupled As_4S_4 and As_4S_3 monomers progressively increasing as x increases to one-half. If the Ge_2S_3 additive were to participate in either reaction ($1c$) or ($2c$) above, one would predict As_4S_4 and As_4S_3 monomers to maximize in concentration near $x = 0.5$ and 0.6 respectively (equations ($1c$) and ($2c$)). In our experiments both reactions take place simultaneously, and if one models these reactions by comparable reaction rates one finds that the concentration of As_4S_4 units displays a *symmetric* profile centred closer to $x = 0.3$, while that of As_4S_3 units shows an *asymmetric* profile centred closer to $x = 1/2$, as found in our experiments. Furthermore, our experiments also reveal that not all of the additive takes part in reactions ($1c$) and ($2c$). Some of the additive forms ethane-like $Ge_2(S_{1/2})_6$ phase in the glasses, the vibrational signature of which is the mode $\nu_7 = 250\ \mathrm{cm}^{-1}$ which first appears near $x = 0.1$ and grows rather rapidly in the glasses once $x > 1/2$.

3.3. Molecular structure of Ge-rich glasses: region II ($0.5 < x < 1.0$)

In region II, the Ge content of the glasses exceeds the As one, and one expects the concentration of As–As bonds (in the two monomers) to steadily decline as the concentration of Ge–Ge bonds (in the form of ethane-like $Ge_2(S_{1/2})_6$) steadily increases. Results of figure 3 show that the ethane-like phase grows in scattering strength rather rapidly once $x > 1/2$. If the ethane-like $Ge_2(S_{1/2})_6$ nanophase were the only molecular phase to occur in the glasses, one would be hard pressed to understand an increase of T_g in region II. For GeS_2 tetrahedra to continue to form in region II a new source of S is required. We believe that a distorted rock-salt-like GeS nanophase formed in the glasses provides the source of S by the following decomposition reaction.

$$Ge_2S_3 = 2GeS + S. \tag{3}$$

The vibrational signature [23, 29] of this nanophase is the mode near 236 cm^{-1} observed in the spectra of figure 3 as a broad band centred near 240 cm^{-1} (ν_7).

Near the chemical composition $x = 0.80$, our results of figure 2(a) show T_g to acquire a global maximum of 446 °C. This value of T_g is quite close to that of pure GeS_2 glass of 508 °C [23]. The somewhat lower T_g of the ternary glass is probably due to the presence of a small concentration of threefold As present in the backbone that lowers the global connectivity and therefore T_g. In the present ternary, the glass composition $x = 0.8$ represents the most connected backbone having the largest mean r. Why does $T_g(x)$ in the ternary glasses decrease at $x > 0.8$?

As x approaches unity the concentration of ethane-like $Ge_2(S_{1/2})_6$ nanophase grows at the expense of the distorted rock-salt GeS, thereby cutting the supply of S needed to promote

growth of GeS_2 phase. In Raman scattering (figure 3) modes in the 200–260 cm^{-1} region become prominent. The mode at 340 cm^{-1} has largely contributions from ethane-like phase as shown by recent first principles cluster calculations [30]. In this range of composition the optical bandgap of the glasses decreases as evidenced by the loss of resonant enhancement in Raman scattering. There is a striking parallel in compositional trends of Raman spectra of the present glasses in the $0.8 < x < 1.0$ range and those of binary Ge_xS_{1-x} glasses [23, 29] in the $1/3 < x < 1/2$ range. The principal features of the microstructure consist of a growth in Ge-rich nanophases at the expense of the GeS_2-like backbone that results in a decrease of T_g. In this range of chemical compositions, the effective global connectivity of the ternary glasses actually *decreases* because the global connectivity of the Ge_2S_3 phase is actually lower [22] than that of GeS_2 phase due to redundant Lagrangian bonding constraints. The behaviour is just the opposite of that one might infer from a simple substitution of x in the formula

$$r = (12 + 2x)/5 \tag{4}$$

describing mean r as a function of x in the present ternary glasses. To summarize, the physical picture of glass structure emerging in region II consists of a conversion of the GeS_2 alloyed As_2S_3 glass network prevailing near $x = 0.5$, to become more connected as Ge for As replacement occurs and an As_2S_3 alloyed GeS_2 backbone emerges. The replacement is facilitated by growth of Ge-rich nanophases in the $0.5 < x < 0.8$ range. At $x > 0.8$, the Ge-rich nanophases grow at the expense of the GeS_2 backbone, as a phase separated Ge_2S_3 glass corresponding to the end-member composition, $x = 1$, is realized.

3.4. Structural anomalies of As–Ge–S glasses near $r = 2.60$

Network glasses can be generically classified in terms of their elastic response [1–3, 43] into *floppy, intermediate and stressed–rigid* phases. The present glasses ($2.4 < r < 2.8$) belong to the *stressed–rigid phase*. The glass forming tendency [44] in the As–Ge–S ternary (figure 6) is rather extensive. The present glasses lie along the As_2S_3 to Ge_2S_3 join, and this region of glass formation is shaded in figure 6 to illustrate the nanoscale phase separated character of their backbones.

The structure of ternary $As_yGe_yS_{1-2y}$ glasses lying along the bisector of the As–S–Ge angle in the ternary composition triangle (figure 6) has been examined in recent Raman, MDSC [45] and EXAFS [46, 47] measurements. These *bisector* glasses (at $y = 0.20$) intersect the present ternary glasses at $x = 1/2$. Compositional trends in $T_g(y)$ for the bisector glasses have also been established [45] by MDSC, and the results appear in figure 7. In this figure we have also projected the T_g variation in binary Ge–S [23] and As–S [48] glasses taken from recent MDSC measurements. One observes a threshold behaviour of T_g in the binary glasses corresponding to stoichiometric (GeS_2, As_2S_3) compositions. In contrast, T_g values of the bisector glasses continue to increase as a function of r, except for a glitch near $r = 2.5$. The latter feature is the result of As–As bonds first appearing in the network near $y = 0.17$ as revealed in Raman scattering measurements [45]. Since these bonds form in As-rich monomers (As_4S_4, As_4S_3) that *decouple* from the backbone, one observes a rather striking reduction of T_g in the narrow compositional window $0.16 < y < 0.20$ due to a loss in global connectivity of the network. At higher concentrations y, fragments of amorphous-As form as S is rapidly depleted from the backbone as will be discussed in a forthcoming publication [45].

The delicate connectivity-related phase transitions in glasses such as rigidity transitions assume, in general, that the underlying backbones are fully polymerized [49] and that changes in global connectivity occur smoothly as a function of chemical composition. At low global connectivities (such as $r < 2.4$), T_g values of binary and ternary glasses are found [43, 50–52],

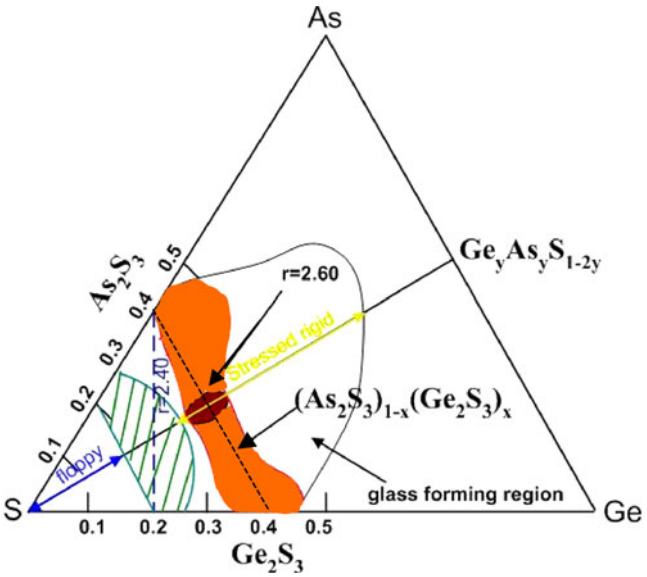

Figure 6. Glass forming region in the As–Ge–S ternary showing the $(Ge_2S_3)_x(As_2S_3)_{1-x}$ join and the $Ge_yAs_yS_{1-2y}$ pathway lying on the bisector of the As–S–Ge angle that cross at $x = 1/2$ corresponding to $r = 2.6$. The brown striped region represents glasses that are phase separated on a nanoscale. In the red region monomers based on As_4S_4 and As_4S_3 are pervasive and result in NSPS of networks. The green striped region represents the intermediate phase.

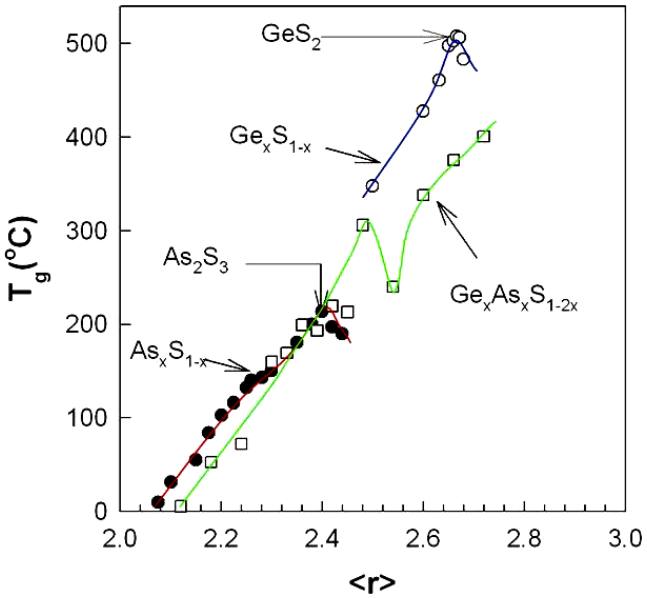

Figure 7. Compositional variation of T_g in binary As_xS_{1-x} ($r = 2+x$) and Ge_xS_{1-x} ($r = 2(1+x)$) and ternary $(Ge_2S_3)_x(As_2S_3)_{1-x}$ glasses ($r = 2 + 3x$). Note that in the binary glasses one observes a global maximum near the chemical thresholds, while in the ternary system T_g continues to increase as a function of r except for a window around 2.55 where nanoscale phase separation (NSPS) occurs and forms a glitch (see text).

in general, to increase monotonically as a function of r largely because these networks are fully polymerized. The anomalies in physical properties of glasses near $r = 2.60$, as shown here, result largely due to the fact that networks at higher r are rarely *completely* polymerized. They usually consist of several nanophases. Structural changes in network glasses can produce gross changes in their physical properties, and can mask the more subtle connectivity-related transitions.

3.5. The special case of ternary As–Ge–Se glasses near $r = 2.60$ and the Tanaka transition

Ternary selenide glasses are of special interest because the nature of structural changes taking place near $r = 2.60$ appears to be qualitatively different from those in corresponding sulfide glasses. Let us first consider the case of ternary $As_yGe_ySe_{1-2y}$ glasses that reside along the bisector of the As–Se–Ge angle in the ternary phase [43, 44, 52] diagram. In these glasses that contain equal concentrations of As and Ge, $T_g(y)$ values are found to increase monotonically [10, 52] with y. Once y exceeds the chemical threshold $y_c = 11/20$, one expects homopolar bonds to emerge. In these selenide glasses it appears that both As–As and Ge–Ge bonds nucleate as part of the backbone [10], thereby increasing the connectedness of the backbone. This is confirmed by trends in $T_g(y)$ that continue to increase even when r exceeds 2.60. These results are in sharp contrast to the glitch observed in corresponding sulfide glasses (figure 7) wherein T_g values decrease by 80 °C as y increases from 0.16 to 0.18. A parallel situation prevails in ternary $P_yGe_ySe_{1-2y}$ glasses where P_4Se_3 monomers decouple from the backbone [53] and a glitch in $T_g(y)$ is observed in the $0.20 < y < 0.23$ range.

The Ge–As–Se bisector glasses are thus ideal test systems to examine the rigidity transition proposed by Keiji Tanaka [19] because nanoscale phase separation effects are qualitatively absent in this ternary. In these glasses, we find evidence [10, 43] of a global minimum in ΔH_{nr} in the $2.30 < r < 2.42$ range associated with self-organization [1, 43] near the Phillips–Thorpe rigidity transition. On the other hand, T_g, ΔC_p or ΔH_{nr} are found to vary smoothly near $r = 2.60$. We find no evidence [10, 40, 43] of anomalies in these thermal parameters that could be identified with a rigidity transition associated with dimensional regression [19].

It is of interest to compare thermal properties of ternary $(Ge_2Se_3)_x(As_2Se_3)_{1-x}$ glasses with corresponding sulfide ones. Compositional trends [54] in T_g for $(Ge_2Se_3)_x(As_2Se_3)_{1-x}$ glasses are plotted in figure 8(a). To afford a quantitative comparison, T_g results on corresponding sulfide glasses (figure 2) are reproduced in figure 8 as well. The overall trends in both glass systems have close similarities displaying a global maximum of T_g near $x = 0.8$. The broken curve in figure 8(a) is a scaled up version of $T_g(x)$ of the selenide glasses by a factor of 1.08. The scaling factor takes into account the higher chemical bond strengths of As–S and Ge–S bonds in relation to As–Se and Ge–Se ones [43, 51, 55]. The broken curve would be a good representation of the variation in T_g in the sulfide glasses if the global connectedness of backbones in the two chalcogenide glasses were similar. The broken curve reproduces the overall T_g variation in the sulfide glasses reasonably well except in the $0.1 < x < 0.6$ region, where the observed T_g values are found to be *systematically lower* (shaded area). The latter is a direct consequence of formation of As-rich monomers in the sulfide glasses that lowers the global connectedness of the remaining backbone reflected in their T_g values. Such effects are clearly absent in the selenide glasses.

The present results also reveal that the widths of the glass transitions, W, near $x = 0.6$ acquire global maxima in *both* ternary glasses (figure 8(b)). The result suggests that W is largely determined by structural heterogeneity of the *network forming* nanophases in both the sulfide and selenide glasses. Clearly, the As-rich monomers do not contribute to W in the X = S glasses since they no longer form part of the backbone. However, growth of Ge-rich

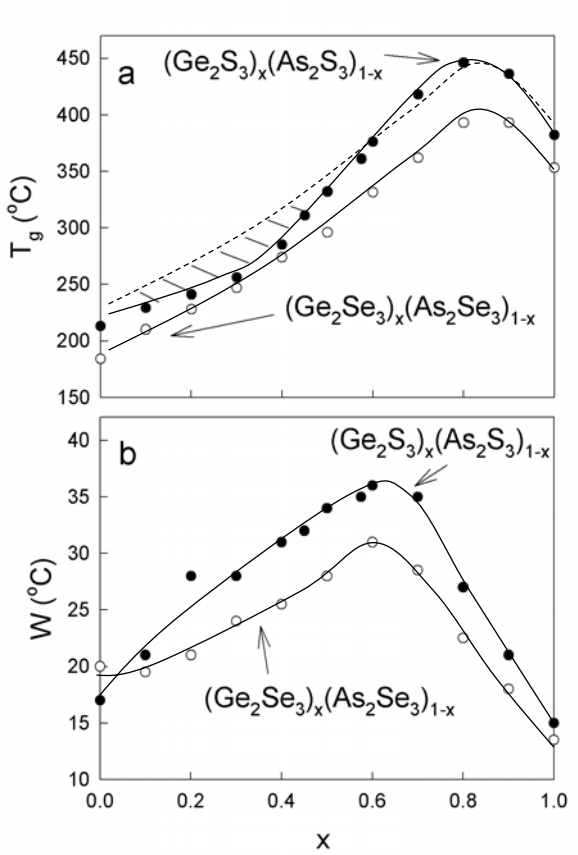

Figure 8. (a) Compositional trends in $T_g(x)$ and (b) glass transition widths, $W(x)$, of $(Ge_2S_3)_x(As_2S_3)_{1-x}$ (●) and $(Ge_2Se_3)_x(As_2Se_3)_{1-x}$ (○) glasses compared. In panel (a) the broken curve is a scaled up (factor of 1.08) plot of the selenide T_g values, and would display the T_g of sulfide glasses if the global connectivity of the two chalcogenide glasses were the same. This is clearly not the case in the $0.1 < x < 0.6$ range for the sulfide glasses where decoupling of As-rich monomers of As_4S_4 and As_4S_3 from the backbone lowers the T_g of the glasses (shaded area). The width of T_g for both systems shows a global maximum near $x = 0.6$ (see text for details).

nanophases based on ethane-like $Ge_2\{(S \text{ or } Se)_{1/2}\}_6$ units and distorted rock-salt Ge(S or Se) units as $x > 1/2$ contribute to heterogeneity of glass structure. In both systems, network structures become structurally heterogeneous near a mean $r = 2.65$ that is reflected in the increased width W of the glass transitions.

4. Conclusions

One can generically classify network glasses in terms of their elastic response into floppy, intermediate and stressed–rigid phases. The present experiments show that stressed–rigid glasses are generally partially polymerized into distinct nanophases. Ternary $(As_2S_3)_{1-x}(Ge_2S_3)_x$ glasses and their selenide counterparts over the glass forming range $(0 < x < 1)$ represent model examples of stressed–rigid networks spanning the $2.4 < r < 2.8$ mean coordination range, and their structure has been examined in Raman scattering and MDSC measurements. At $x = 0$, the network structure consists of an As_2S_3-like backbone with a small but finite concentration of As_4S_4 monomers *nanoscale phase separated* from

the backbone. As x increases to one-half or r to 2.60, the Ge_2S_3 additive alloys largely as GeS_2 in the As_2S_3 backbone with S provided by precipitation of As-rich phases of As_4S_4 and As_4S_3 monomers. These monomers segregate *qualitatively* from the backbone and lower the global connectedness of the backbone as reflected in T_g values. The latter can be seen when results on corresponding selenide glasses are compared to those on the present sulfides. In the $0.5 < x < 0.8$ range, the additive continues to alloy as GeS_2 in the As_2S_3 backbone but this time by precipitating a (Ge-rich) distorted rock-salt-like GeS phase as T_g values increase to acquire a global maximum near $x = 0.8$. At still higher x (>0.8), the Ge_2S_3 additive enters the glass network largely as an ethane-like phase leading to a rapid loss of the GeS_2–As_2S_3 backbone and reduction of T_g values. These structure results suggest that anomalies in sulfide glasses near $r = 2.60$ can be traced to nanoscale phase separation of As-rich monomers in stressed–rigid networks.

Acknowledgments

It is a pleasure to acknowledge the assistance of Dr H Schaeffer in the Raman scattering experiments, and discussions with Dr E Vateva and Dr E Skordeva. This work is supported by NSF grant DMR-01-01808.

References

[1] Boolchand P, Georgiev D G and Goodman B 2001 *J. Optoelectron. Adv. Mater.* **3** 73
[2] Phillips J C 2000 *Phys. Rev. Lett.* **88** 216401
[3] Thorpe M F, Jacobs D J, Chubynsky M V and Phillips J C 2000 *J. Non-Cryst. Solids* **266–269** 859
[4] Kerner R and Phillips J C 2001 *Solid State Commun.* **117** 47
[5] Rader A J, Hespenheide B M, Kuhn L A and Thorpe M 2002 *Proc. Natl Acad. Sci. USA* **99** 3540
[6] Phillips J C 2000 *Phil. Mag.* B **80** 1773
[7] Selvanathan D, Bresser W J and Boolchand P 2000 *Phys. Rev.* B **61** 15061
[8] Feng X, Bresser W J and Boolchand P 1997 *Phys. Rev. Lett.* **78** 4422
[9] Georgiev D G, Boolchand P and Micoulaut M 2000 *Phys. Rev.* B **62** R9228
[10] Qu T, Georgiev D G, Boolchand P and Micoulaut M 2003 *Supercooled Liquids, Glass Transition and Bulk Metallic Glasses (Mater. Res. Soc. Symp. CC vol 754)* (Boston, MA: Materials Research Society) at press
[11] Georgiev D G, Boolchand P, Eckert H, Jackson K and Micoulaut M 2003 *Europhys. Lett.* **62** 49
[12] Wang Y, Wells J, Georgiev D G, Boolchand P, Jackson K and Micoulaut M 2001 *Phys. Rev. Lett.* **87** 5503
[13] Boolchand P, Georgiev D G and Micoulaut M 2002 *J. Optoelectron. Adv. Mater.* **4** 823
[14] Boolchand P, Feng X and Bresser W J 2001 *J. Non-Cryst. Solids* **293** 348
[15] Phillips J C 1979 *J. Non-Cryst. Solids* **34** 153
[16] Thorpe M F 1983 *J. Non-Cryst. Solids* **57** 355
[17] Boolchand P and Thorpe M F 1994 *Phys. Rev.* B **50** 10366
[18] Boolchand P, Zhang M and Goodman B 1996 *Phys. Rev.* B **53** 11488
[19] Tanaka K 1989 *Phys. Rev.* B **39** 1270
[20] Kerner R and Micoulaut M 1997 *J. Non-Cryst. Solids* **210** 298
[21] Micoulat M and Naumis G 1999 *Europhys. Lett.* **47** 568
[22] Boolchand P and Bresser W J 2000 *Phil. Mag.* B **80** 1757
[23] Cai L and Boolchand P 2002 *Phil. Mag.* B **82** 1649
[24] Boolchand P 2000 *Asian J. Phys.* **9** 709
[25] Velinov T, Gateshki M, Arsova D and Vateva E 1997 *Phys. Rev.* B **55** 11014
[26] Arsova D, Skordeva E, Nesheva D, Vateva E, Perakis A and Raptis C 2000 *Glass Phys. Chem.* **26** 247
[27] Nesheva D and Skordeva E 1999 *Phys. Status Solidi* a **172** 149
[28] Georgiev D G, Boolchand P and Jackson K A 2003 *Phil. Mag.* B at press
[29] Boolchand P, Grothaus J, Tenhover M, Hazle M A and Grasselli R K 1986 *Phys. Rev.* B **33** 5421
[30] Jackson K A, Briley A, Grossman S, Porezag D V and Pederson M R 1999 *Phys. Rev.* B **60** R14985
[31] Lucovsky G, Nemanich R J and Galeener F L 1977 *Amorphous and Liquid Semiconductors* (Edinburgh: University of Edinburgh) p 130

[32] Myers M B and Felty E J 1967 *Mater. Res. Bull.* **2** 535
[33] Ward A 1968 *J. Raman Spectrosc.* **72** 4133
[34] Tanaka K, Gohda S and Odajima A 1985 *Solid State Commun.* **56** 899
[35] Sklenar S, Vlcek M and Bezdicka P 1999 *Proc. 5th ESG Conf. on Glass Science and Technology for 21st Century* p 108
[36] Effey B and Cappelletti R L 1999 *Phys. Rev.* B **59** 4119
[37] Frumar M, Polak Z and Cernosek Z 1999 *J. Non-Cryst. Solids* **256/257** 105
[38] Pauling L 1960 *Nature of the Chemical Bond* (Ithaca, NY: Cornell University Press)
[39] Zallen R and Slade M L 1978 *Phys. Rev.* B **18** 5775
[40] Muniz-Miranda M, Sbrana G, Bonazzi P, Menchetti S and Pratesi S 1996 *Spectrochim. Acta* A **52** 1391
[41] Ystenes M, Brockner W and Menzel F 1993 *Vib. Spectrosc.* **5** 195
[42] Mamedov S and Mikhailov M D 1997 *J. Non-Cryst. Solids* **221** 181
[43] Boolchand P, Georgiev D G, Qu T, Wang F, Cai L and Chakravarty S 2002 *C. R. Chimie* at press
[44] Borisova Z U 1981 *Glassy Semiconductors* (New York: Plenum)
[45] Qu T and Boolchand P 2003 unpublished
[46] Aitken B and Ponader C W 2000 *J. Non-Cryst. Solids* **274** 124
[47] Sen S, Ponader C W and Aitken B G 2001 *Phys. Rev.* B **64** 1042902
[48] Georgiev D G 2003 *PhD Thesis* University of Cincinnati
[49] Thorpe M F, Jacobs D J and Djordjevic B R 2000 *Insulating and Semiconducting Glasses* ed P Boolchand (Singapore: World Scientific) p 95
[50] Tatsumisago M, Halfpap B L, Green J L, Lindsay S M and Angell A C 1990 *Phys. Rev. Lett.* **64** 1549
[51] Micoulaut M 2002 *Europhys. Lett.* **58** 830
[52] Wang Y, Boolchand P and Micoulaut M 2000 *Europhys. Lett.* **52** 633
[53] Chakravarty S, Micoulaut M and Boolchand P 2003 unpublished
[54] Georgiev D G, Mamedov S, Qu T and Boolchand P 2003 unpublished
[55] Tichy L and Ticha H 1999 *Phil. Mag.* B **79** 373